Available online at www.sciencedirect.com
SCIENCE DIRECT®
ELSEVIER
Photonics and Nanostructures – Fundamentals and Applications xxx (2004) xxx–xxx
PHOTONICS AND NANOSTRUCTURES
Fundamentals and Applications
www.elsevier.com/locate/photonics

All-optical diode in an asymmetrically apodized Kerr nonlinear microresonator system

Suresh Pereira[a], Philip Chak[b,*], J.E. Sipe[b], Lasha Tkeshlashvilli[c,d], Kurt Busch[c,d]

[a]*Centre d'optique, photonique et laser, Université Laval, Sainte-Foy, Que., Canada G1K 7P4*
[b]*Department of Physics, University of Toronto, 60 St. George Street, Toronto, Ont., Canada M5S 1A7*
[c]*Institut für Theorie der Kondensierten Materie, Universität Karlsruhe, 76128 Karlsruhe, Germany*
[d]*Department of Physics and School of Optics, CREOL & FPCE, University of Central Florida, Orlanda, FL 32816, USA*

Received 3 May 2004; received in revised form 4 August 2004; accepted 4 August 2004

Abstract

We show numerically that a Kerr nonlinear system composed of two channel waveguides coupled periodically by circular microresonators can be used as an all optical diode. The diode has low intensity requirements (~ 50 MW/cm^2) and compact dimensions (~ 100 μm).

PACS: 42.65.T

Keywords: Microresonator; Nonlinear pulse propagation

1. Introduction

Among the driving forces in the study of nonlinear optics in waveguiding structures is the possibility of constructing fast, efficient devices for use in all-optical computation, or in the routing of signals for telecommunications. To this end, various authors have proposed devices based on nonlinear switching in periodic, Kerr nonlinear media [1–3]. Such devices have often been discussed with an implementation in Bragg gratings [3,4] in mind. These gratings possess photonic band gaps (PBGs), which are frequency regions in which light of low intensity cannot propagate. Light of high intensity, though, can form into a gap soliton and propagate through (or switch out of) the structure [4,5]. The excitation of a gap soliton involves balancing the group velocity dispersion (GVD) experienced by light with the self phase modulation (SPM) induced by a Kerr nonlinearity [5]. Unfortunately, Bragg gratings typically exhibit enormous GVD at the frequency ranges where switching should occur, so the switching intensity can be quite large. However, it has recently been theoretically predicted [6] that side-coupled microresonator structures

* Corresponding author. Tel.: +1 416 978 6185; fax: +1 416 723 9302.
E-mail address: pchak@physics.utoronto.ca (P. Chak).

1569-4410/$ – see front matter
doi:10.1016/j.photonics.2004.08.004

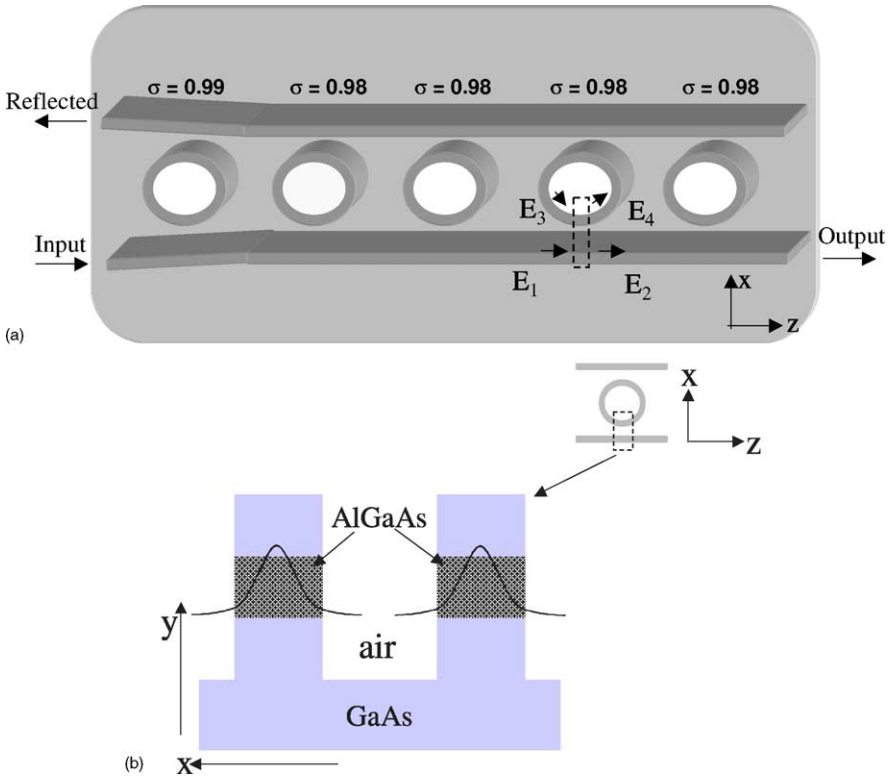

Fig. 1. (a) Schematic of the microresonator structure (top–down view). The left-most resonator has a larger self-coupling coefficient ($\sigma = 0.99$) than the other resonators. A typical coupling point is indicated by the dotted rectangle. Also indicated is the field configuration used in the coupling matrix given in the text. (b) Cross-section of the channel waveguide. The light is confined in the AlGaAs region by air in the lateral (x) direction, and by AlGaAs in the transverse (y) direction.

(Fig. 1a—top–down view; Fig. 1b—cross-section), which consist of two channel waveguides periodically coupled by microresonators, exhibit two types of PBGs: a familiar Bragg gap associated with the periodicity of the structure; and a *resonator* gap, associated with the resonant frequency of the microresonators (see Fig. 4a). The two types of gap have very different properties. Specifically, the GVD experienced by light with frequency content slightly outside a resonator gap can be orders of magnitude smaller than the GVD slightly outside a Bragg gap. Since the energy required for gap soliton formation scales with the GVD [7], gap soliton effects should occur at a much lower intensity in resonator gaps than in Bragg gaps [6]; hence, microresonator structures can potentially be used for low-intensity nonlinear logical operations such as all-optical AND gates [11] and optical memory [12].

In this paper we propose a side-coupled microresonator structure as an all-optical diode, a device that transmits light of a given frequency and intensity in only one direction. The basic device operation is as follows. Light travelling in the forward (backward) direction in the lower channel waveguide is coupled, via the microresonators, to light travelling in the backward (forward) direction in the upper channel waveguide. In general this coupling is quite weak, but when the carrier frequency of the light is close to an integer multiple of the resonant frequency, ω_r, of the microresonators, then the effect of the coupling is enhanced, and a resonator stop gap opens in the transmission spectrum [6]. However, in the presence of a Kerr nonlinearity, light of high intensity can form into a gap soliton, and hence transmit through the resonator stop gap [6], which leads to intensity-dependent switching. It has been shown that switching

behaviour in a Kerr nonlinear structure is facilitated by apodization [6], that is, by making the coupling to the first and last resonators slightly weaker than the coupling to the middle resonators, hence allowing light to 'ease into' the structure. It is this observation that leads to the construction of our diode. We apodize only the left-most microresonator so that light incident from the left can 'ease into' the structure, and will switch at a lower intensity than light incident from the right. We show below that for a certain range of intensities, light incident from the left is partially transmitted, while light incident from the right is almost fully reflected.

The theoretical and experimental feasibility of all-optical diodes in a variety of geometries has been investigated. Dowling et al. [23,24] proposed a diode in a Bragg structure composed of alternate stacks of linear and Kerr nonlinear media. Mingaleev and Kivshar [8] investigated the feasibility of an all-optical diode in a Kerr nonlinear photonic crystal waveguiding structure using optical bistability. An experimental demonstration of an all-optical diode using a quasi-phase matching technique, was realized by Gallo et al. [10]. We believe that our diode proposal has some significant advantages over these other proposals, notably because of its simplicity and low energy requirements.

In Section 2 of this paper we discuss the numerical technique that we use to model light propagation in the resonator structure. In Section 3 we discuss the general linear properties of finite and infinite microresonator structures. In Section 4 we apply the numerical technique to the diode structure, and discuss our results.

2. Device modeling

Linear properties of microresonator structures can be modelled using finite-difference, time domain (FDTD) simulations [13]. In FDTD simulations the full Maxwell equations are used to simulate the propagation of a short pulse through the structure, generating a transmitted and reflected pulse. By comparing the Fourier transforms of the transmitted and reflected light to that of the incident light, the transmission/reflection spectrum of the structure can be determined. However, such simulations are intensely time-consuming, and are therefore not amenable to the solution of nonlinear problems in microresonator structures. The difficulty with using FDTD to solve nonlinear problems is two-fold. First, in nonlinear problems the device operation is intensity-dependent, so the FDTD simulation must be re-run for each intensity being used. Second, the different frequencies in a pulse interact nonlinearly, so a simulation run with, say, 10 ps pulses does not necessarily give insight into device operation using 100 ps pulses. Consequently, in this paper we use an approximate numerical technique to model device operation. The model includes all of the relevant physics, and can reproduce the results of the FDTD for linear device operation [13].

We model the propagation of light in two steps. First, we note that typical resonators are fabricated in AlGaAs and confined in the lateral direction by air (Fig. 1b). The large index contrast between AlGaAs ($n \simeq 3$) and air means that the waveguide modes are tightly confined in the lateral direction to the AlGaAs region. We therefore assume, as is common [14,15], that evanescent tail coupling between the channel waveguides and the resonators occurs only at the points of smallest separation between them. We call these points (one of which is indicated schematically by the rectangle in Fig. 1a) the 'coupling points'. Away from the coupling points, the light is confined to a mode of either the waveguide or the resonator, and hence the primary consequence of propagation is the accumulation of linear and nonlinear phase, and linear and nonlinear loss. To describe this propagation we define a field, $A(\zeta, t)$, which represents the amplitude of the guided mode at position ζ and time t, with $\zeta = z$ in the channel waveguides, and $\zeta = R\theta$ in the microresonators, where R is the microresonator radius, and θ is the polar angle. The field $A(\zeta, t)$ is normalized such that its square modulus gives the intensity of light in the mode. We characterize the linear phase accumulation of the mode using an effective index of refraction, n_{eff}, assumed to be equal for the channel waveguides and the microresonators. Furthermore, we assume that n_{eff} is independent of frequency, which amounts to ignoring the material dispersion of the system; this is justified because the dispersion time for 100 ps pulses at 1.55 μm in typical AlGaAs structures is about 70 ns [16], while in this paper we consider time-scales of about 1 ns. We

characterize self-phase modulation (SPM) using a nonlinear index of refraction coefficient, n_2, and we ignore other nonlinear effects, such as third harmonic generation, which are not phase matched, and hence should play a negligible role in the field dynamics. The effects of linear loss, two-photon absorption and three-photon absorption, are characterized by the coefficients α_1, α_2 and α_3, respectively. With these approximations, the field evolution is described by [6]

$$\frac{1}{\delta\zeta}A(\zeta,t+\delta t)=\left(\frac{1}{\delta\zeta}+i\frac{\bar{\omega}}{c}[n_{\text{eff}}+n_2 I]\right)A(\zeta-\delta\zeta,t)-\frac{1}{2}(\alpha_1+\alpha_2 I+\alpha_3 I^2)A(\zeta-\delta\zeta,t), \quad (1)$$

where $\delta\zeta$ and $\delta t=\delta\zeta/(c/n_{\text{eff}})$ are the discretization length- and time-steps, $\bar{\omega}$ is the carrier frequency, and $I\equiv|A(\zeta-\delta\zeta,t)|^2$. In writing Eq. (1) we have assumed that the mode profile of light is strongly localized within the waveguide core, as is common in semiconductor waveguiding structures.

When light impinges on a coupling point, we describe the coupling between the channel waveguides and the resonators by a matrix. Using this approach, we assume [14,15] that the coupling is well-described by a self- (σ) and a cross- (κ) coupling coefficient. Furthermore, we assume that there is no reflection at the coupling points, so that the fields E_i (a typical set is shown in Fig. 1a) are related via

$$\begin{bmatrix}E_4\\E_2\end{bmatrix}=\begin{bmatrix}\sigma & i\kappa\\ i\kappa & \sigma\end{bmatrix}\begin{bmatrix}E_3\\E_1\end{bmatrix}. \quad (2)$$

To conserve energy we require $|\sigma|^2+|\kappa|^2=1$ and $\sigma^*\kappa=\sigma\kappa^*$. We have used the approach of Rowland and Love [17] to estimate the intensity dependence of the strength of σ and κ; the indicated dependence, for the coupling geometries and materials that we consider, is negligible. Therefore, we assume that there is no nonlinearity in a small region around the coupling points, which simplifies the numerics without affecting the basic physics. For a given structure, the values of σ and κ can be determined by FDTD simulations [13], or by a modified coupled mode theory [17].

3. Linear properties of the resonator structure

In this section we discuss the general linear properties of our structure. We start by simulating the linear properties of a two-channel microresonator device in the absence of loss ($\alpha_{1,2,3}=0$). We assume that $n_{\text{eff}}=3$, which is appropriate for AlGaAs [18]. We consider resonators with circumference $2\pi R=26$ μm, for which the fundamental resonant frequency is $\omega_r=c/(n_{\text{eff}}R)$, and the 50th resonance occurs at a vacuum wavelength $\lambda=1.56\,\mu$m. In the absence of nonlinearity, the reflection spectrum of channel waveguides coupled by a *single* resonator is well described by a Lorentzian lineshape [19]:

$$r=\frac{(-1)^{N+1}\gamma e^{i\phi}}{\gamma-i\Delta}, \quad (3)$$

where N indexes the resonance, $\Delta=\omega-N\omega_r$ is the frequency detuning from the Nth resonance, ϕ accounts for the phase accumulated in the waveguides, and $2\pi\gamma=\omega_r(1-\sigma^2)/\sigma^2$ is the width of the resonance. In Fig. 2 we plot the reflectivity ($|r|^2$) of a single resonator with $\sigma=0.98$ (solid line) and $\sigma=0.99$ (dashed line). The reflection spectrum of the resonator with $\sigma=0.98$ is slightly wider, since the smaller value of σ (self-coupling) implies a larger value of κ (cross-coupling). The reflection spectra are accompanied by a Lorentzian build-up of the intensity in the microresonators relative to the intensity in the channel waveguide. To quantify this build-up we define I_i as the intensity of the incident light in the channel

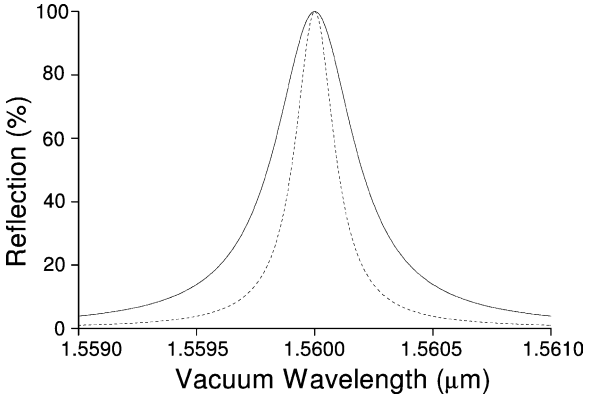

Fig. 2. Linear reflection spectrum for two channel waveguides coupled by a single resonator with self-coupling coefficient $\sigma=0.98$ (solid line) and $\sigma=0.99$ (dashed line).

waveguide, and $I_{\rm res}$ as the intensity of the field inside the resonator respectively. We then find that for $\sigma \simeq 1$, the intensity build-up in the resonator is:

$$\frac{I_{\rm res}}{I_{\rm i}} = \frac{(1-\sigma^2)}{(1-\sigma^2)^2 + (4\pi^2\sigma^2\Delta^2/\omega_{\rm r}^2)}. \tag{4}$$

At the resonant frequency ($\Delta = 0$), this build-up is $1/(1-\sigma^2)$, so that with small coupling between the ring and waveguide ($\sigma \simeq 1$) the intensity enhancement inside the resonator is increased. The generalization of Eq. (4) in the presence of Kerr nonlinearity has been presented, and the effect of bistability investigated [19]. It has been shown that for a positive Kerr nonlinearity bistability only occurs when $\Delta < 0$. For $\Delta > 0$ no bistability occur within the intensity range of interest.

For a series of resonators each spaced by a distance d the propagation Eq. (1) and the coupling matrix (2) can be combined into a transfer matrix [6]. Without loss of generality we assume that light travels in the forward (backward) direction in the lower (upper) channel waveguide. In Fig. 3 we sketch a series of resonators. Since the resonators are spaced by d we can, as in Fig. 3, divide the structure into a series of unit cells of width d, with the resonator in the middle of the cell. We then define a frequency-dependent amplitude $l_n^{\rm i}(\omega)$ ($u_n^{\rm i}(\omega)$) that gives the strength of the field entering the nth unit cell ($l_n^{\rm i}$ is at the bottom left corner of the cell, $u_n^{\rm i}$ is at the upper right corner) at the input (left-most point); and an amplitude $l_n^{\rm o}(\omega)$ ($u_n^{\rm o}(\omega)$) that gives the strength of the field leaving the nth unit cell. Combining the propagation Eq. (1) and the coupling matrix (2) we find that these amplitudes are related via

$$\begin{bmatrix} l_n^{\rm o}(\omega) \\ u_n^{\rm o}(\omega) \end{bmatrix} = \frac{1}{t_n}\begin{pmatrix} t_n^2 - r_n^2 & r_n \\ -r_n & 1 \end{pmatrix}\begin{bmatrix} l_n^{\rm i}(\omega) \\ u_n^{\rm i}(\omega) \end{bmatrix}, \tag{5}$$

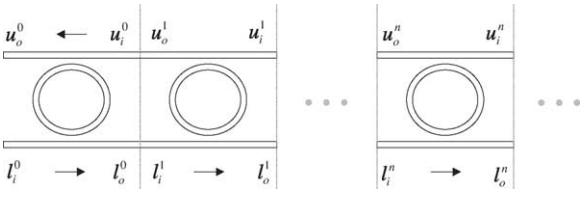

Fig. 3. Schematic for a series of resonators, the resonators are spaced by distance d.

where, in the Lorentzian approximation discussed above [19],

$$r_n = (-1)^{(N+1)}\frac{\gamma_n e^{i\phi_n}}{\gamma - i\Delta},$$
$$t_n = -i\frac{\Delta e^{i\phi_n}}{\gamma_n - i\Delta},$$

where γ_n is the Lorentzian coupling coefficient in the nth unit cell, $\phi_n = n_{\rm eff}\omega d/c$ is the phase accumulated in the waveguides in the nth cell, Δ is the frequency detuning from the Nth resonance, and the factor $(-1)^{N+1}$ is related to the symmetry of the resonator mode. Because the resonance-width parameter (γ_n) can vary from cell to cell, the transfer matrix approach can be used to describe finite structures with arbitrary apodization.

The transfer matrix (5) can be used to determine the dispersion relation of an infinite, periodic micro-resonator structure. Applying Bloch's theorem to our fields, we impose the usual condition that the output fields differ from the input fields only by a phase [9],

$$\begin{bmatrix} l_n^{\rm o}(\omega) \\ u_n^{\rm o}(\omega) \end{bmatrix} = e^{ik_{\rm eff}d}\begin{bmatrix} l_n^{\rm i}(\omega) \\ u_n^{\rm i}(\omega) \end{bmatrix}.$$

Clearly $e^{ik_{\rm eff}d}$ is an eigenvalue of (5), so the dispersion relation, $\omega(k_{\rm eff})$, can be determined using

$$\begin{vmatrix} t_n^2 - r_n^2 - t_n e^{ik_{\rm eff}d} & r_n \\ -r_n & 1 - t_n e^{ik_{\rm eff}d} \end{vmatrix} = 0.$$

In Fig. 4a we plot this dispersion relation for the material parameters listed above, with $\sigma = 0.96$ and a unit cell spacing $d = 16\,\mu$m. On Fig. 4a we label two distinct types of photonic band gaps: a resonator gap, which opens at integer multiples of the resonant frequency, $\omega_{\rm r} = c/(n_{\rm eff}R)$; and a Bragg gap at integer multiples of the Bragg frequency, $\omega_{\rm b} = \pi c/(n_{\rm eff}d)$. The two gaps are qualitatively different. The resonator gap is indirect, which means that the top and bottom edges of the gap occur at different values of the effective wavenumber; by contrast, the Bragg gap is direct. For both types of gap, the first derivative of the dispersion relation vanishes at the band edges, so the group velocity of light at the band edges is zero. However, the bands around the resonator gap are much flatter, which means that the group velocity dispersion experienced by light at the edge of a resonator gap is

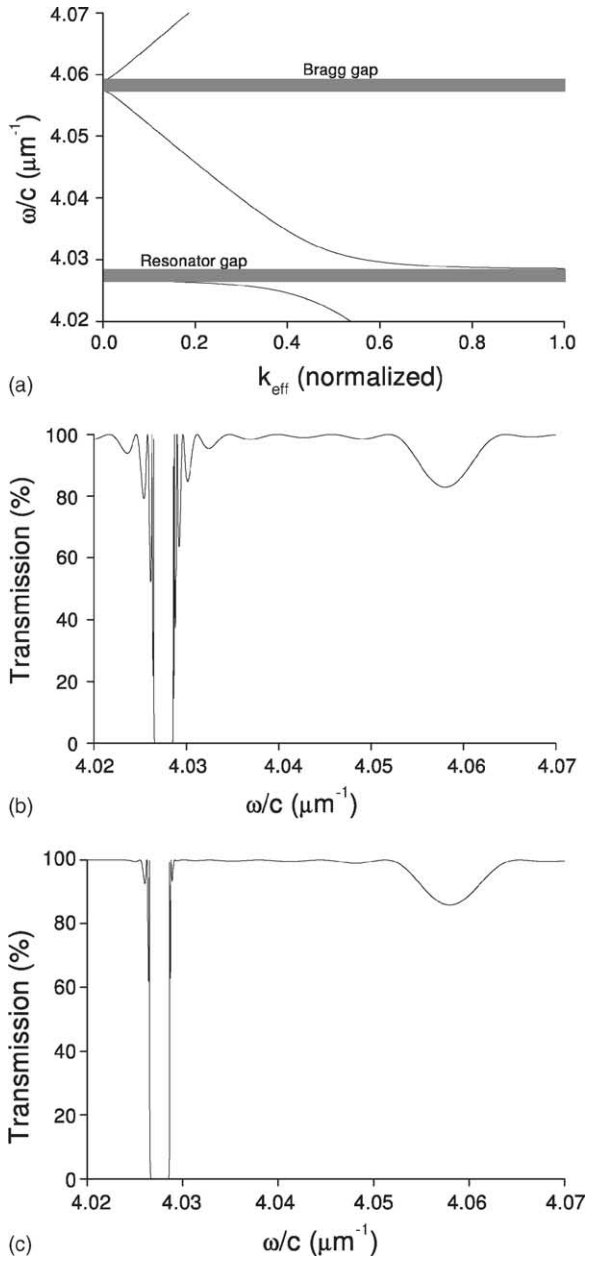

Fig. 4. (a) Dispersion relation for a two channel microresonator structures with $2\pi R = 26\,\mu\text{m}$, $d = 16\,\mu\text{m}$, $n_{\text{eff}} = 3.0$ and $\sigma = 0.96$. (b) Transmission for finite structure with 10 resonators, all unit cells have $\sigma = 0.96$. (c) Transmission for finite, apodized structure with 10 unit cells, first and last unit cells have $\sigma = 0.98$, all other unit cells have $\sigma = 0.98$.

significantly smaller than the GVD for light at the edge of a Bragg gap. In fact, the GVD at the edge of the resonator gap depicted in Fig. 4a is approximately 300 times smalled that at the Bragg gap in the Figure. Since gap soliton formation involves the balancing of the GVD at the band edge with a Kerr nonlinearity, the pulse intensities required for gap soliton effects in a resonator gap are substantially lower than in a Bragg gap [6]. We discuss these gap soliton effects further in Section 4.

While the dispersion relation gives an excellent qualitative understanding of pulse propagation in the microresonator structures, in practice all structures are finite. In Fig. 4b we plot the transmission spectrum for a structure with 10 unit cells, each with a self-coupling coefficient $\sigma = 0.96$. The stop-gap in Fig. 4b aligns with the predicted resonator gap for the infinite structure in Fig. 4a. However, at the edges of the gap there are huge oscillations in the transmission of the finite structure, caused by Fabry-Perot effects at the first and last microresonators [6]. The Fabry-Perot effects can be minimized by apodizing the structure – that is, gradually increasing the value of σ for the first and last sets of resonators. In practice, the required variation in coupling can be achieved by slightly curving the waveguide, as indicated in Fig. 1a, such that the distance between the waveguides and the resonator varies with position. Since the value of the coupling coefficients is based on evanescent tail coupling, an increase in separation distance will increase the self coupling (σ), and decrease the cross coupling (κ). In Fig. 4c we plot a transmission spectrum using a symmetric apodization profile, such that $\sigma = 0.96$ except for the first and last resonator, which have $\sigma = 0.98$. Notice that the ripples in the transmission spectrum are much smaller than in the un-apodized case, because the impedance mismatch for light entering the system is smaller for a resonator with $\sigma = 0.98$ than it is for a resonator with $\sigma = 0.96$.

Finally, we note that the length scale required for observation of a resonator gap in a finite structure is much smaller than that required to observe a Bragg gap. In Fig. 4a there is a Bragg gap predicted at $\omega/c = 4.058\,\mu\text{m}^{-1}$. However, in the transmission spectra for the finite structures (4b,c) this Bragg gap appears as only a very slight dip in the transmission. Close to the centre of the resonator stop gap at $\omega/c = 4.03$ of Fig. 4b the transmission drops to 10^{-40},

while for the Bragg stop gap it drops only to 0.8. One requires tens or even hundreds of resonators to observe a significant stop gap near a Bragg frequency of the structure [6]. However, as shown in Fig. 2, a single resonator is sufficient to give zero transmission in the vicinity of a resonant frequency of the resonators; furthermore, a gap with a reasonably flat transmission spectrum requires only two or three resonators [6].

4. Numerical simulations and discussion

We now consider two types of diode structures. The first consists of twenty resonators, apodized such that the leftmost resonator has $\sigma = 0.99$, and all the other resonators have $\sigma = 0.98$. The second consists of five resonators, such as shown in Fig. 1a, where the leftmost resonator has $\sigma = 0.99$, and the other four have $\sigma = 0.98$. In both structures the resonators are spaced by 16 μm. For each structure, one can consider the transmission spectrum associated with light incident from either end. In the linear limit, it follows from the general properties of quasi-one-dimensional structures that the two spectra will be the same. In Fig. 5 we plot the linear transmission spectrum of the two diode structures. The dashed line gives the spectrum of a structure with twenty resonators, while the solid line gives the spectrum of the five resonator structure. Both spectra exhibit a photonic stop gap at about $\lambda = 1.56\,\mu$m. The

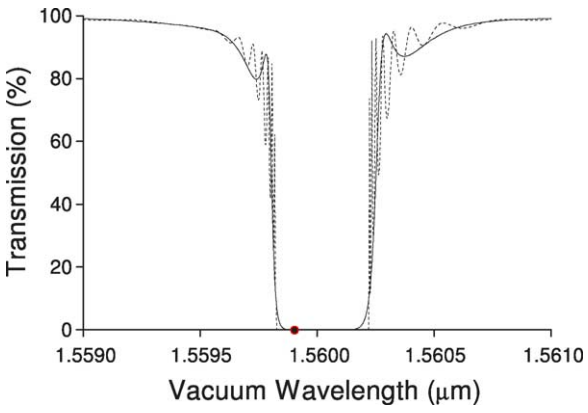

Fig. 5. Linear reflection spectrum for a 20 cell (dashed line) and 5 cell (solid line) diode structure, apodized as discussed in the text. The large dot in the stop gap shows the carrier frequency used for the nonlinear simulations.

oscillations at the edges of the stop gap are an unavoidable consequence of our asymmetric apodization profile [6]. As discussed in the previous section, in a symmetric structure these resonances could be further minimized, but then the diode operation of the device in the nonlinear regime would vanish.

Although the transmissivity of our structure is almost zero for low intensity light within the stop gap, for light of high intensity the transmissivity can be significantly increased. This increased intensity is caused by the phase accumulation induced by the Kerr nonlinearity, which shifts the light away from the resonance condition of the microresonators, and hence reduces the reflectivity. In Bragg gratings, this process is sometimes referred to as gap soliton formation [5]. A similar process occurs in the stop gap of our resonator structure [11], although the nonlinear dynamics of the pulse that propagates through the resonator gap is less well understood. As discussed in the previous section, a single resonator is sufficient to give zero transmission (albeit only for a single wavelength; see Fig. 2). Consequently, one can discuss the formation of a nonlinear excitation that propagates in the stop gap created by a single resonator. With reference to Fig. 2, it is clear that this nonlinear excitation can be formed at a lower input intensity in the resonator with $\sigma = 0.99$, since its resonance is narrower *and* its intensity build-up (Eq. (4)) is higher. Therefore, light injected into the diode structure from the left hand side (into the $\sigma = 0.99$ resonator) can somewhat adiabatically transform into the appropriate gap excitation for propagation through the other four resonators. Conversely, light injected from the right hand side, into the $\sigma = 0.98$ resonator, requires a larger input intensity to form the appropriate nonlinear excitation.

We verify the above by simulating pulse propagation through our structure in the presence of a Kerr nonlinearity using $n_2 = 1.1 \times 10^{-4}$ rm cm^2/GW, and nonlinear loss parameters $\alpha_2 = 0.05$ cm/GW and $\alpha_3 = 0.08$ cm^3/GW^2, all of which are typical values for AlGaAs [18]. However, we have verified that for the intensity ranges discussed below, the effects of nonlinear loss are minimal. Far more important is the linear loss, α_1. To demonstrate this, in Fig. 6a and b we plot the transmission of the 20 cell and 5 cell structures respectively, as a function of the intensity of light injected from the left-hand side of the structure. We

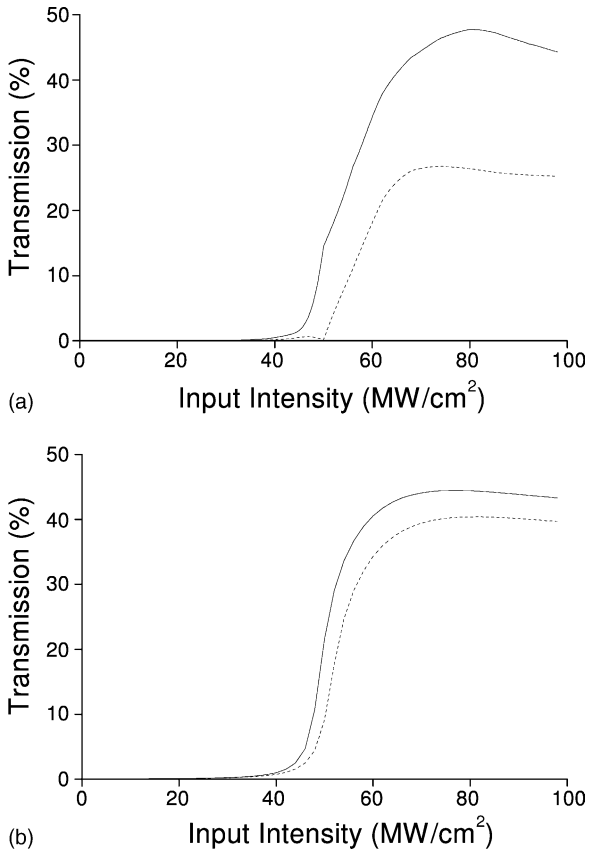

Fig. 6. Transmissivity as a function of incident intensity for light incident from the left for (a) a 20 cell structure and (b) a 5 cell structure. In both plots the solid line gives the transmission in the absence of loss, and the dashed line simulation assumes a linear loss $\alpha_1 = 0.16\,\mathrm{cm}^{-1}$ which corresponds to 0.7 dB/cm.

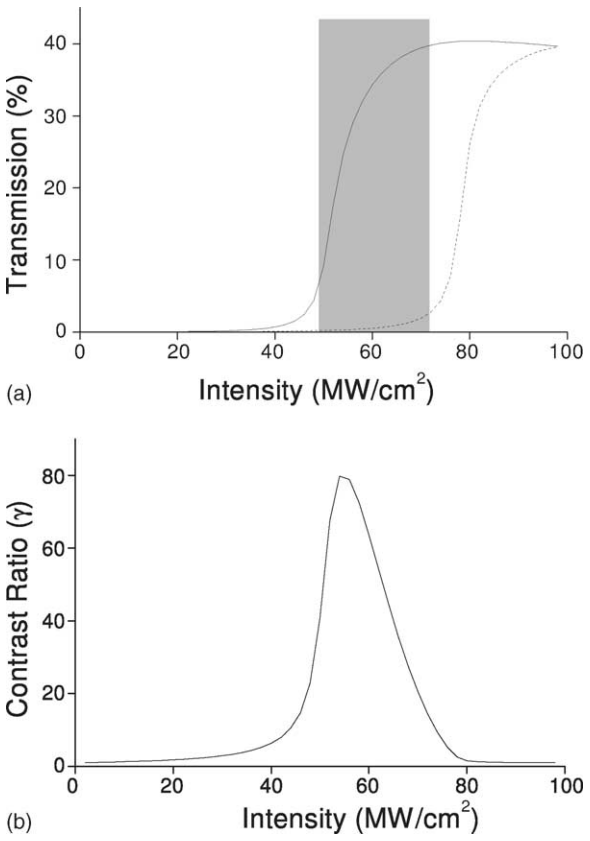

Fig. 7. Five cell structure: (a) nonlinear transmission as a function of input intensity for light incident from the left (solid line) and the right (dashed line); (b) contrast ratio γ (defined in the text) as a function of incident intensity.

use Gaussian pulses with intensity full-width, half-maximum (FWHM) of 100 ps. We assume a carrier wavelength of 1.5599 μm which is in the stop gap of both structures (it is indicated by the large dot in Fig. 5), with $\Delta > 0$, so that the bistability does not occur within our intensity range of interest. In both 6a and b the solid line represents the transmission in the absence of linear loss ($\alpha_1 = 0$), and the dashed line represents the transmission when $\alpha_1 = 0.16\,\mathrm{cm}^{-1}$ (which corresponds to an intensity loss of 0.7 dB/cm). For both structures, linear loss is detrimental, but in the 5 cell structure the peak transmission is reduced only by about 9%, while in the 20 cell structure it is reduced by almost 45% relative to the value in the absence of loss. Note that since the 20 cell structure is only about 320 μm long, with $\alpha_1 = 0.16\,\mathrm{cm}^{-1}$ one might naively expect a loss of about $0.022\,\mathrm{dB} \simeq 0.5\%$. The simulated loss of 45% corresponds to an effective loss coefficient of 70 dB/cm, which is 100 times large than the assumed loss parameter. This enhanced loss is due to the fact that light with frequency content in the stop gap of the structure circulates many times through the structure, so the effective distance that light travels is much larger than the length of the channel waveguides. Consequently, in the following we concentrate on the 5 cell structure.

In Fig. 7a we plot the transmission through the 5 cell structure for light incident from the left (solid line) and the right (dashed line) as a function of the peak intensity of the incident pulse, using $\alpha_1 = 0.16\,\mathrm{cm}^{-1}$. In the shaded intensity range (about 50–70 MW/cm^2),

light from the left experiences significant transmission, while light from the right is almost completely reflected; this intensity range constitutes the region of diode operation for our device. To characterize this we define a contrast ratio, γ, as the ratio of transmitted energy when light is incident from the left to the transmitted energy when light is incident from the right; this gives a measure of how effectively the diode distinguishes a logical 'one' from a logical 'zero'. In Fig. 7b we plot γ as a function of the intensity of the incident pulse. The peak contrast ratio $(\gamma = 80)$ occurs at an incident intensity of 56 MW/cm^2. By choosing a carrier frequency which gives lower transmission in the linear regime we could substantially enhance γ, but at the expense of a higher switching threshold. In Fig. 8 we plot the transmitted pulse for light incident from the left for an input intensity of 60 MW/cm^2. This transmitted light has a slightly asymmetric profile due to the frequency and intensity dependence of the group delay inside the structure. Furthermore, because of self-phase modulation it is compressed by a factor of about 3, which means that although the energy transmission is 34%, the peak transmitted *intensity* is about 90% of the peak incident intensity. As a consequence of this compression, the frequency spectrum of the pulse is broadened by a factor of about 3. Finally, we note that although our device is only 80 μm long, the delay between the input and the transmitted pulse is about 70 ps, so that the group delay experienced by the transmitted light is about 100 times larger than in a straight waveguide of the same length. This enhanced group delay, and the consequent enhancement of the effect of the Kerr nonlinearity, is primarily responsible for the low operating intensity for our device.

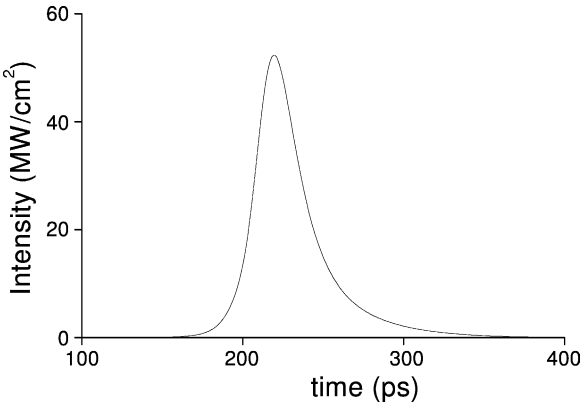

Fig. 8. Output pulse shape for light incident from the left of the structure with incident intensity 60 MW/cm^2.

The main limitation of our proposed diode is linear loss in the structure. This linear loss has two sources: radiation loss induced by the bend in the microresonators [20]; and scattering loss caused by imperfections in the etching of the channel waveguides and resonators. While the bending loss in typical AlGaAs resonators is typically very small [20], the scattering loss in presently fabricated AlGaAs resonators can reach about 58 dB/cm (13.25 cm^{-1}) [20,21]. However, it is to be expected that as the fabrication process matures, this loss will reach more manageable levels. We have chosen $\alpha_1 = 0.16\,\mathrm{cm}^{-1}$ for the microrings, which is slightly larger than the scattering loss in straight AlGaAs waveguides [22] and hence seems to be a reasonable target value. In the absence of linear loss, the contrast ratio is about 100 for a 5 cell structure, and 180 for a 20 cell structure. Therefore, if the losses can be controlled, a longer structure is more effective.

The diode structure that we propose in this paper has several attractive features including a low operating intensity, compact dimensions (<100 μm), excellent contrast ratio and good energy transmission. We note that the nonlinear diode previously proposed by Dowling and coworkers [23,24], based on a Bragg stack geometry, is competitive with our proposal. While our structure has better energy transmission and a cleaner output pulse, the Bragg stack geometry has a smaller operating intensity. However, the Bragg stack proposal has the significant drawback that its construction requires the complicated growth of alternating stacks of linear and Kerr nonlinear materials. The structure that we propose in this paper is based on the rapidly developing technology of microring resonators, and may thus be easier to fabricate. Highly efficient two-channel microresonator structures have been fabricated [25]; and researchers have observed the enhancement of nonlinear effects in one-channel structures [26] and two-channel structures [21]. As regards the diode experimentally demonstrated by Gallo et al. [10] in a quasi phase matched system, we note that it used 20 ns pulses, rather than the more telecommunications-friendly 100 ps pulses in our scheme; furthermore, the threshold power for their

diode operation was 1.6 W, whereas our diode operates about about 50 MW/cm^2 which, given a typical effective mode area of $\sim 1.0\,\mu m^2$ for a microresonator in AlGaAs, translates to about 0.5 W.

In closing, we note that although we have concentrated on circular microresonators in conventional waveguiding structures, it has been demonstrated theoretically that side-coupled resonators can be fabricated in photonic crystal (PC) waveguiding structures [27]. In principle, PC structures can be infiltrated with nonlinear materials, and hence should be able to support the diode operation described in this paper.

Acknowledgements

P.C. acknowledges funding from an Ontario Graduate Scholarship; S.P. and J.E.S. acknowledge funding from the Natural Sciences and Engineering Research Council of Canada, and J.E.S. from Photonics Research Ontario. K.B, L.T. and S.P. acknowledge support by the Deutsche Forschungsgemeinschaft (DFG) through the DFR-Forschungszentrum ''Functional Nanostructures'' (DFG-CFN). The research of L.T. and K.B. is further supported by DFG-project No. Bu 1107/2-3 (Emmy-Noether program). S.P. thanks Sergei Mingaleev for helpful discussions.

References

[1] H.G. Winful, G.D. Cooperman, Appl. Phys. Lett. 40 (1982) 298.
[2] S. Lee, S.T. Ho, Opt. Lett. 18 (1993) 962.
[3] D. Taverner, N.G.R. Broderick, D.J. Richardson, M. Ibsen, R.I. Lamming, Opt. Lett. 23 (1998) 259.
[4] B.J. Eggleton, R.E. Slusher, C.M. de Sterke, P.A. Krug, J.E. Sipe, Phys. Rev. Lett. 76 (1996) 1627.
[5] C.M. de Sterke, J.E. Sipe, Progress in Optics, in: E. Wolf (Ed.), Amsterdam, North-Holland, 1994, p. 203.
[6] S. Pereira, P. Chak, J.E. Sipe, J. Opt. Soc. Am. B 19 (2002) 2191.
[7] S. Pereira, J.E. Sipe, J. Heebner, R.W. Boyd, Opt. Lett. 27 (2002) 536.
[8] S.F. Mingaleev, Y.S. Kivshar, J. Opt. Soc. Am. B 19 (2002) 2241.
[9] J. Heebner, Philip Chak, Suresh Pereira, J.E. Sipe, R.W. Boyd, J. Opt. Soc. Am. B 21 (9) (2004).
[10] K. Gallo, G. Assanto, K.R. Parameswaran, M.M. Fejer, Appl. Phys. Lett. 79 (2001) 314.
[11] S. Pereira, P. Chak, J.E. Sipe, Opt. Lett. 28 (2003) 444.
[12] P. Chak, J.E. Sipe, S. Pereira, Opt. Lett. 28 (2003).
[13] A. Taflove, S.C. Hagness, Computational Electrodynamics—The Finite-difference Time-domain Method, Artech House Publishers, 2000.
[14] J.E. Heebner, R.W. Boyd, Q-H. Park, J. Opt. Soc. Am. B 19 (2002) 722.
[15] D. Rafizadeh, J.P. Zhang, S.C. Hagness, A. Taflove, K.A. Stair, S.T. Ho, R.C. Tiberio, Opt. Lett. 22 (1997) 1244.
[16] M.A. Afromowitz, Solid State Commun. 15 (1974) 59.
[17] D.R. Rowland, J.D. Love, IEE Proc. J. Optoelectron. 14 (1993) 177.
[18] A. Villeneuve, C.C. Yang, P.G.J. Wigley, G.I. Stegeman, J.S. Aitchison, C.N. Ironside, Appl. Phys. Lett. 61 (1992) 147.
[19] P. Chak, J.E. Sipe, S. Pereira, Opt. Commun. 213 (2002) 163.
[20] V. Van, P.P. Absil, J.V. Hryniewicz, P.T. Ho, J. Lightwave Tech. 19 (2001) 1734.
[21] J.E. Heebner, N.N. Lepeshkin, A. Schweinsberg, G.W. Wicks, R.W. Boyd, R. Grover, P.-T. Ho, Opt. Lett. 29 (2004) 769.
[22] K. Al-hemyari, A. Villeneuve, J.U. Kang, J.S. Aitchison, C.N. Ironside, G.I. Stegeman, App. Phys. Lett. 63 (1992) 3582.
[23] M. Scalora, J.P. Dowling, C.M. Bowden, M.J. Bloemer, J. Appl. Phys. 76 (1994) 2023.
[24] M.D. Tocci, M.J. Bloemer, M. Scalora, J.P. Dowling, C.M. Bowden, Appl. Phys. Lett. 66 (1995) 2324.
[25] C.-Y. Chao, L. Jay Guo, J. Vac. Sci. Technol. B 6 (2002) 2862.
[26] P.P. Absil, J.V. Hryniewicz, B.E. Little, P.S. Cho, R.A. Wilson, L.G. Joneckis, P.T. Ho, Opt. Lett. 25 (2000) 554.
[27] S. Fan, P.R. Villenevue, J.D. Joannopoulos, M.J. Khan, C. Manolatou, H.A. Haus, Phys. Rev. B 59 (1999) 15882.